Biophysical Journal Volume 66 May 1994 1542–1553

Kinetic Mechanism of Myofibril ATPase

Yong-Ze Ma and Edwin W. Taylor
Department of Molecular Genetics and Cell Biology, University of Chicago, Chicago, Illinois 60637 USA

ABSTRACT The kinetic mechanism of myofibril ATPase was investigated using psoas and mixed back muscle over a range of ionic strengths. Myofibrils were labeled with pyrene iodoacetamide to measure the rate constants for the binding of ATP and formation of the weakly attached state. The velocity of shortening was measured by stopping the contraction at various times by mixing with pH 4.5 buffer. The transient and steady-state rates of ATP hydrolysis were measured by the quench flow method. The results fitted the kinetic scheme

$$\underset{}{\overset{(1)}{}} \quad \overset{(2)}{} \quad \overset{(3)}{} \quad \overset{(4,\,-P)}{} \quad \overset{(5)}{} \quad \overset{(6)}{}$$
$$AM + ATP \rightleftharpoons AM(ATP) \rightleftharpoons AM \cdot ATP \rightleftharpoons AM \cdot ADP \cdot P \longleftrightarrow AM' \cdot ADP \rightleftharpoons AM(ADP) \rightleftharpoons AM + ADP.$$

The rate constants (or equilibrium constants for steps 1 and 6) were obtained for the six steps. k_5 was calculated from the K_M for shortening velocity, K_1, and k_2. The rate constants were essentially equal for myofibrils and acto-S-1 at low ionic strength. Increasing the ionic strength up to 100 mM in NaCl increased the rate of the hydrolysis step and the size of the phosphate burst and the effective rate of product release became the rate-limiting step. The step size calculated from the velocity of shortening, k_5, and k_2 is 15 nm, based on a model in which step 4 is the force-generating step.

INTRODUCTION

The kinetic mechanism of actomyosin ATPase has been extensively studied in solution, and the scheme is a basis for models of contraction (Hibberd and Trentham, 1986). Most of the studies were done with single-headed myosin subfragment 1 at very low ionic strength, because the interaction of the proteins at the higher physiological ionic strength is weak. It could be argued that some properties of the system may be significantly different at higher ionic strength. In addition, the association-dissociation steps are second-order reactions in solution, but they are pseudo-first order in the muscle lattice or in motility assays.

These objections can be met by determining the kinetic behavior of whole fibers using caged ATP (Goldman et al., 1984) and by studies of myofibrils (White, 1985; Hermann et al., 1992; Houadjeto et al., 1992). The two systems are complementary. Fibers have the advantage that the effect of tension on rate processes can be studied while myofibrils permit more accurate measurements of several steps in the mechanism, including the hydrolysis reaction. The aim of the present work is to determine the rate constants for the steps in the cycle for myofibrils and to compare the values of the constants with acto-S-1. The dependence of the rates of some steps of the ATPase cycle on strain in the actomyosin complex has been included in contraction models since the original mechanochemical theory of Huxley (1957). A finding of the present studies with myofibrils undergoing unloaded shortening is that for the steps that were measured, namely the binding of ATP and isomerization of the ATP-actomyosin complex, the hydrolysis step and the steps in product dissociation, the values of the rate constants are approximately the same as the values for acto-S-1 in solution at the same ionic strength.

Several recent studies have addressed the problem of the distance moved per ATP hydrolyzed. Very large distances, >100 nm (Harada et al., 1990; Ishijima et al., 1991), intermediate values of 50–60 nm (Higuchi and Goldman, 1991), and values of 10–20 nm (Uyeda et al., 1990; Uyeda et al., 1991; Pate et al., 1993a,b) have been reported. Values larger than 20 nm exceed the distance that could be spanned in the conventional rotating cross-bridge model. The rate constants of the kinetic scheme and the velocity of shortening allow a calculation of the step size from a simple mechanochemical model. The value is ~15 nm and, although it depends to some extent on the choice of model, the kinetic data appear to be consistent with the conventional model.

MATERIALS AND METHODS

Protein and myofibril preparation

Actin, pyrene-labeled actin, myosin, and subfragment-1 were prepared by methods described previously (Rosenfeld and Taylor, 1987; Taylor, 1991). In the case of psoas muscle, relatively large amounts of actin are released in the myosin extraction step. The actin was removed by two centrifugations in the presence of 25 mM MgATP. Myosin thick filaments were prepared by dialysis of myosin from 0.6 M NaCl to 0.1 M NaCl (10 mg/ml myosin, 25 mM PIPES buffer, pH 7, 1 mM EGTA, 2 mM $MgCl_2$). The filaments were further dialyzed against the salt concentration and buffer used in the experiment. Myofibrils were prepared from rabbit psoas and mixed back muscles. To prepare myofibrils for shortening velocity measurements, the muscle was cut into thin strips which were stretched to 1.2–1.3 times rest length and tied to plastic rods. The strips were soaked overnight in rigor buffer (20 mM Tris-Mes, pH 7.0, 0.1 mM potassium acetate, 5 mM EGTA, 2 mM 2-mercaptoethanol, 0.1 mM phenylmethylsulfonyl fluoride, 1 mM NaN_3) plus 0.5% Triton X-100. The fibers were finely chopped and homogenized in 5 volumes of rigor buffer using an Omnimixer to give mainly

Received for publication 9 June 1993 and in final form 11 February 1994.

Address reprint requests to Dr. Edwin W. Taylor, Department of Molecular Genetics and Cell Biology, Cummings Life Science Center, The University of Chicago, 920 East 58th Street, Chicago, IL 60637. Tel.: 312-702-1620; Fax: 312-702-3172; E-mail: ewtl@midway.uchicago.edu.

0006-3495/94/05/1542/12 $2.00

single myofibrils. These were washed five times by centrifugation and filtered through cheesecloth followed by passage through 70-μm and then 30-μm nylon mesh filters. In the case of stretched fibers used for velocity measurements, only the central part of the strip was used in the preparation to improve the homogeneity in sarcomere length. The length was 2.2 μm for unstretched and 2.6–2.8 μm for stretched samples. Stretched myofibrils were used in most biochemical experiments on psoas, but stretching did not produce significant differences; in earlier experiments with back muscle, the myofibrils were prepared at rest length.

Cross-linked myofibrils were prepared by reacting with 10 mM 1-ethyl-3-(3-dimethylaminopropyl)-carbodiimide in rigor buffer for 10–20 min at 20°C. The reaction time was determined as the minimum that prevented shortening by ATP in the presence of calcium. The cross-linked myofibrils were essentially unregulated by calcium.

The myofibrils were stored in rigor buffer at 4°C and generally used within a few days. In most experiments the ionic strength was varied by centrifugation and resuspension of myofibrils in buffer containing various concentrations of NaCl (25 mM PIPES, pH 7.0, 1 mM EGTA, 2 mM $MgCl_2$). Some experiments were done using sodium acetate or KCl to vary the ionic strength but no significant differences were found. In earlier experiments myofibrils were prepared from rabbit back muscle and stored in 50% glycerol-rigor buffer at −20°C before use.

The myosin concentration in myofibril suspensions is difficult to measure accurately. Based on densitometry of SDS-PAGE gels stained with Coomassie brilliant blue, the myosin content is 0.5 of the total protein. A value of 0.43 has been commonly used (Yates and Greaser, 1983). Measurement of concentration is affected by the tendency of myofibrils to clump and stick to surfaces and the failure to completely dissolve for colorimetric assays. An extinction coefficient of 7.0 at 280 nm for 1% solution of myofibrils in 2% SDS has been used by most investigators (Sutoh and Harrington, 1977). Calibration curves prepared from mixtures of actin and myosin to simulate the ratio in myofibrils gave an extinction coefficient of 10 for 1% solution in SDS. The concentration was also measured using BCA reagent (Pierce, Rockford, IL) in 1% SDS calibrated using mixtures of actomyosin. The two methods agreed within 10%. The differences in calibration of protein concentration, myosin content, and myosin molecular weight could lead to a 20% difference in the values for molar concentrations used by various investigators.

Pyrene-labeled myofibrils

N-(1-pyrinyl)-iodoacetamide in dimethylsulfoxide was added to myofibrils at a 5:1 ratio to the actin content and reacted overnight at 4°C (25 mM PIPES buffer, pH 7.0, 100 mM NaCl, 2 mM $MgCl_2$, 1 mM EGTA). Dithiothreitol, final concentration 2 mM, was added to stop the reaction, and unreacted label which had partially precipitated was adsorbed to cellulose CF-11 added at 1% (w/v). Cellulose was removed by gentle centrifugation. Myofibrils were washed by centrifugation or dialyzed against the same buffer used for the labeling reaction but with the addition of 1 mM dithiothreitol and a NaCl concentration of 50 mM. Different labeling conditions were investigated. Reaction for 1 hour at room temperature and 5 h at 4°C or reaction overnight at a 10:1 ratio of label to actin gave a similar degree of labeling and a similar relative change in fluorescence by ATP.

Kinetic studies

The binding of ATP was measured by the change in fluorescence of pyrene myofibrils (excitation 365 nm; emission 405 nm) using the stop-flow apparatus described previously (Taylor, 1991). The apparent second-order rate constant was also measured for the binding of methylanthranyloyl ATP (16).

The phosphate burst and early steady-state phase of ATP hydrolysis was measured using a quench flow apparatus. The machine was rebuilt during the course of these experiments to provide better thermostating of the samples. The two Berger mixers were replaced with offset "T" mixers because it was found that myofibrils were broken and stretched by the shear gradients in the Berger mixers which were also more subject to clogging by aggregates of myofibrils. There was some loss in time resolution but, based on the phosphate burst for S-1, the lag in the hydrolysis reaction is 3 ms, which is an upper limit for the mixing time. In myofibril reactions the lag in the phosphate burst was <4 ms. The similar duration of the lag indicates that diffusion into the myofibrils is not affecting the reaction rate. The degree of hydrolysis of the ATP[γ-^{32}P] was determined as the fraction of phosphate counts to total counts by separation of nucleotide from phosphate on charcoal columns. The procedure has been described (Sadhu and Taylor, 1992).

Shortening velocity

The method of Ohno and Kodama (1991) was used to measure the velocity of shortening. Myofibrils were mixed with ATP in the quench flow apparatus just as for phosphate burst experiments, and shortening was stopped by mixing with 0.4 M sodium acetate, pH 4.5, instead of 3 N PCA. Myofibril length was measured using a 63X Zeiss planapochromat phase contrast lens in a Nikon Optiphot microscope. The image was displayed on a TV monitor using a Javelin CCD camera. Measurements were made by placing a grid on the TV screen. Magnification was calibrated using a Leitz micrometer slide. Microscope slides were prepared, and for each time point the lengths of about 30 myofibrils containing at least 5 sarcomeres each were measured. In early experiments 2% glutaraldehyde was added to the stopping solution (Ohno and Kodama, 1991), but it did not improve the image and increased the clumping. Mixing with sodium acetate and then ATP 10 ms later produced sarcomere spacing that was the same as the control. Therefore the low pH blocks shortening in <10 ms.

The length versus time curves appeared to extrapolate back to the length at zero time. The relatively large standard error in the measurements of sarcomere length is primarily caused by the variation in sarcomere length of the preparation of stretched myofibrils. The standard error in length of the preparation of rigor myofibrils was similar to myofibrils that had been passed through the quench flow apparatus.

Properties of pyrene-labeled myofibrils

The myofibrils were labeled with pyrene iodoacetamide to assay for the rate of ATP binding. The two- to threefold quenching of the fluorescence of pyrene-labeled actin by the binding of myosin heads is reversed by dissociation of the actomyosin by ATP (Kouyama and Mihashi, 1981). However, reaction of myofibrils or acto-S-1 with the pyrene label directed to sulfhydryl groups will label other myofibril cysteine residues besides the Cys-374 of actin. The specificity and side effects of labeling had to be determined before the label could be used to measure ATP binding.

The reaction of myofibrils in rigor with a sulfhydryl reagent increases the labeling of actin and decreases the labeling of myosin SH groups as compared to labeling under relaxing conditions (Duke et al., 1976). SDS-PAGE gels of pyrene-labeled myofibrils showed, in addition to the fluorescence of actin, an emission from myosin heavy chain, from the tropomyosin-troponin-I region and from bands at 100 kDa and 130 kDa. The distribution of label is similar to that reported by Duke et al. (1976). Pyrene-labeled polymeric actin has an anomalous absorption at 365 nm in addition to the absorption maximum for protein derivatives at 344 nm (Kouyama and Mihashi, 1981). Purified actin, purified S-1, and the complex of the two proteins were labeled under the same conditions as myofibrils. The stoichiometry of labeling of actin and S-1 was 0.7–0.9 mol/mol based on absorbance at 344 nm. For actin the fluorescence emission at 405 nm was 1.5 times larger for excitation at 365 nm as compared with 344 nm, whereas for S-1 the emission was reduced to 0.4 of its value at 344 nm. Thus for comparable labeling of the two proteins, the emission is four times larger for actin when excited at 365 nm. Labeling of a 1:1 actin-S-1 complex followed by separation of the S-1 showed that the label on S-1 was reduced to 0.2 mol/mol, while the extent of labeling of the actin was unchanged. The fluorescence properties of the S-1 labeled in a rigor complex were different from the S-1 labeled in the absence of actin. In the latter case, the fluorescence increased 30–50% for the binding of ATP and decreased 10% for the binding of actin, while the S-1 obtained by labeling of the acto-S-1 complex gave a <5% change in fluorescence with ATP or actin. If acto-S-1

is a model for the labeling reaction of rigor myofibrils, the label on the myosin will not appreciably contribute to the fluorescence change produced by the binding of ATP.

Myofibrils were labeled in rigor and fractionated by extraction with high salt to prepare actomyosin and the myosin was separated from the actin by centrifugation in presence of 20 mM Mg ATP. Native tropomyosin was separated from the actin by extraction with 0.8 M NaCl. The specific fluorescence of the actin corresponded to 0.3–0.4 mol of label per mole of actin and the fluorescence was quenched twofold by the binding of S-1.

The myosin preparation contained some actin which has a higher fluorescence per weight of protein. After correction for actin content, the myosin fluorescence corresponded to about 0.3 mol/mol of heavy chain. This myosin gave at most a 10% change in fluorescence for the addition of ATP or actin; part of the change is from actin contamination. Thus the fluorescence properties of the actin and myosin labeled in myofibrils are similar to those of acto-S-1 labeled as a rigor complex in solution.

The contribution of the label on troponin-tropomyosin to the myofibril fluorescence was <5%. From these experiments it is concluded that although the labeling is not specific for actin, ~90% of the change in fluorescence for excitation at 365 nm is contributed by the actin component.

The actual signal obtained by mixing myofibrils with ATP is small (~10–15% change), since about two-thirds of the actin does not have myosin bound to it. However, it contributes to the fluorescence, and there is also a background fluorescence from label on other proteins. As expected, the addition of S-1 to saturate the actin binding sites increased the amplitude of the signal obtained by mixing with ATP by a factor of 2–2.5.

The steady-state ATPase, velocity of shortening, and degree of regulation by Ca for labeled and unlabeled myofibrils were not significantly different.

Analysis of kinetics

The data are analyzed in terms of the scheme

$$\begin{array}{ccccccccc} & & (1) & & (2) & & (3) & & (4,-P) \\ AM + T & \rightleftharpoons & AM(T) & \rightleftharpoons & AM\cdot T & \rightleftharpoons & AM\cdot D\cdot P & \longleftrightarrow & AM'\cdot D \\ & & & & \updownarrow & (3') & \updownarrow & & \\ & & & & M\cdot T & \rightharpoonup & M\cdot D\cdot P & & \end{array} \qquad (1)$$

$$\begin{array}{ccccc} & & (5) & & (6) \\ & \rightharpoonup & AM'\cdot(D) & \rightharpoonup & AM + D. \end{array}$$

For each step, rate and equilibrium constants are defined: $k_3/k_{-3} = K_3$, etc. Step 4 is probably made up of two transitions, an isomerization followed by rapid release of phosphate (Dantzig et al., 1992). The scheme is not a theory but a minimum description of the reaction in terms of intermediates that have been identified.

Much of the kinetic theory has been given in previous papers and is summarized here. The first two steps, ATP binding and isomerization, are measured by the enhancement of pyrene fluorescence in step 2. The data fitted a single exponential term, and the rate constant increased according to a hyperbolic relation. The apparent rate constant is $q = K_1k_2[ATP]/(K_1[ATP] + 1)$ (Johnson and Taylor, 1978). The reversal of step 2 is neglected because the rate of the next step is large. The initial slope of a plot of q vs. ATP concentration defines the apparent second-order rate constant k'. Since the maximum rate k_2 is ~1000 s^{-1} and the weakly bound states dissociate very rapidly in muscle, the association-dissociation of M·T and M·D·P can be treated as rapid equilibria relative to the hydrolysis and product release steps 3 and 4. At a high ATP concentration such that $q > k_3$, the transient and steady-state phases of hydrolysis can be represented by scheme 2:

$$E\cdot T \underset{k_{-3}}{\overset{\bar{k}_3}{\rightleftharpoons}} E\cdot D\cdot P \overset{\bar{k}_e}{\rightharpoonup} E + D + P$$

$$\text{where} \quad E\cdot T = AM\cdot T + M\cdot T$$

$\bar{k}_3$ is the average forward rate constant of step 3, $\bar{k}_3 = f_T k_3 + (1 - f_T)k'_3$, where f_T is the fractional association of ATP states and similarly for $\bar{k}_{-3}$. The average effective rate constant for dissociation of products is $\bar{k}_e$. Since the rate constant can be neglected for the dissociated state, $\bar{k}_e = f_{D\cdot P}k_e$. It has been shown (Rosenfeld and Taylor, 1984) that transient rate constant of the phosphate burst λ, the size of the phosphate burst B, and the steady-state rate V are given by: $\lambda = \bar{k}_3 + \bar{k}_{-3} + \bar{k}_e$, $B = (\bar{k}_3 - V)/\lambda$, $V = \bar{k}_3\bar{k}_e/\lambda$, respectively. The three equations can be solved to obtain the rate constants $\bar{k}_3$, $\bar{k}_{-3}$, and $\bar{k}_e$. It is shown that K_6 is a rapid equilibrium step; therefore $\bar{k}_e = \bar{k}_4k_5/(\bar{k}_4 + k_5)$.

The dissociation constant of ADP was obtained from the inhibition of the rate of ATP binding to pyrene-labeled myofibrils for a range of ADP concentrations. It is assumed that ADP is in rapid equilibrium with myosin sites with dissociation constant K_D. Since the fraction of free sites is $1/(1 + [ADP]/K_D)$, the apparent second-order rate constant for ATP binding is reduced by this factor. The slope of a double reciprocal plot of rate and ATP concentration is $(1 + [ADP]/K_D)/k'$, and the value of K_D was obtained from a secondary plot of the slopes versus ADP concentration.

The solution for the case that the ADP dissociation step is not in rapid equilibrium gives two exponential terms for the time course of ATP binding with rate constants k_5 and $k_2K_1[ATP]/(1 + K_1[ATP] + [ADP]/K_6)$. The data fitted a single exponential term which is consistent with a large value for K_5, so that the AM′·ADP is not present at equilibrium.

Velocity of shortening

A constant velocity of shortening requires the force per cross-bridge to be 0 averaged over a large number of cross-bridge cycles. It is assumed that only strongly bound states contribute to the force, that a strain d is generated by the transition from AM·D·P to AM′·D, and that the head remains attached until the AM·T state is reached, which dissociates immediately. τ is the lifetime of the strongly attached states. $\tau = 1/k_5 + 1/q$, since the AM(T) and AM(D) are rapid equilibria and their contributions can be neglected. At a saturating ATP concentration $\tau_{Min} = 1/k_5 + 1/k_2$. The force is initially αd and at time t it is $\alpha(d - Ut)$, where U is the velocity of shortening and α is the stiffness. The condition of zero force is

$$0 = \alpha \int_0^\infty (d - Ut)\exp\left(-\frac{t}{\tau}\right) dt$$

which gives $U = d/\tau$. Therefore d can be obtained from k_2, k_5, and U_{Max}, where U_{Max} is the velocity at saturating ATP concentration.

The dependence of U on ATP concentration is obtained from $U/U_{Max} = \tau_{Min}/\tau$. Substitution of the rate constants and rearrangement gives $U/U_{Max} = [ATP]/(K_M + [ATP])$, where $K_M = k_5/k'(1 + k_5/k_2) = 1/(k'\tau_{Min})$. The value of d can also be obtained from $U_{Max} = dK_Mk'$.

This simple model has been used to determine d from actin filament velocity using the equation $U = dV/r$, where r is the duty cycle ratio. Since r is τ_{Min}/τ_{cyc} and the ATPase cycle time is $1/V$, this equation for U is equivalent to $U = d/\tau$.

The simple model approximates the decay of force-generating states by a single decay time. Since there is a lag in force decay arising from the transition from AM′ · D to AM, the correct expression for the decay is $[q\exp(-k_5t) - k_5\exp(-qt)]/(q - k_5)$. Substitution into the integral equation gives $U = d(k_2k_5)[(k_2)^2 - (k_5)^2]/[(k_2)^3 - (k_5)^3]$ at saturating ATP. Since k_2/k_5 is in the range of 2–4, the value of d calculated from this equation is ~20% smaller than given by the simple model. Also, the dependence of velocity on ATP concentration departs slightly from a hyperbola.

RESULTS

Binding of ATP to myofibrils

The fluorescence signal obtained by mixing pyrene-labeled myofibrils with ATP in the stop-flow apparatus is shown in Fig. 1. The signal was well fitted by a single exponential term. If there is a lag phase for diffusion of ATP into the myofibril, it is within the dead time of 2 ms.

The rate constant for the fit to a single exponential was determined over a range of ATP concentrations from 25 μM

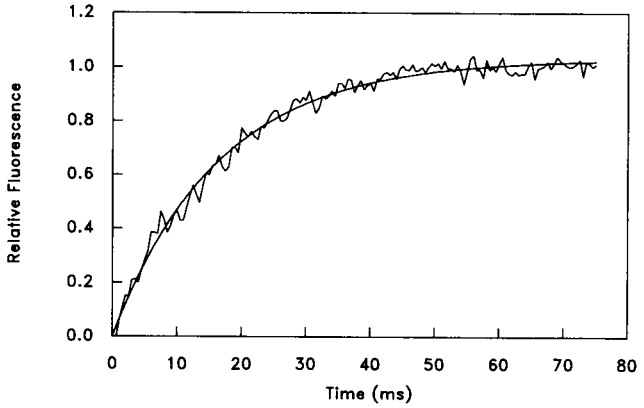

FIGURE 1 Time course of the enhancement of fluorescence for the binding of ATP to pyrene-labeled myofibrils. The smooth curve is the computer-generated fit to one exponential term, rate constant 60 s^{-1}. Conditions, 20°C, 25 mM PIPES buffer, pH 7.0, 50 mM NaCl, 2 mM Mg Cl_2, 1 mM EGTA, 0.4 mg/ml psoas myofibrils, 20 μM MgATP (concentrations after mixing).

to 2.5 mM. A typical data set obtained at 20°C and 50 mM NaCl is plotted in Fig. 2. The data are consistent with a two-step reaction,

$$AM + ATP \overset{K_1}{\rightleftharpoons} AM(ATP) \overset{k_2}{\rightleftharpoons} AM \cdot ATP$$

where K_1 is an equilibrium constant for a rapid weak binding step and k_2 is the rate constant for isomerization to a state of enhanced fluorescence. The initial slope of the plot defines the apparent second-order rate constant, $k^a = K_1k_2$. The data fit a hyperbola as required by this mechanism with a maximum rate k_2 of ~1000 s^{-1} at 20°C.

The rate constants for myofibrils were compared with those for acto-S-1 for a range of temperatures (Table 1). The values of k^a and k_2 agreed within 50%. Although the rate constant k_2 is ~30% smaller for myofibrils than for acto-S-1, the difference is probably within the errors in extrapolation of the data.

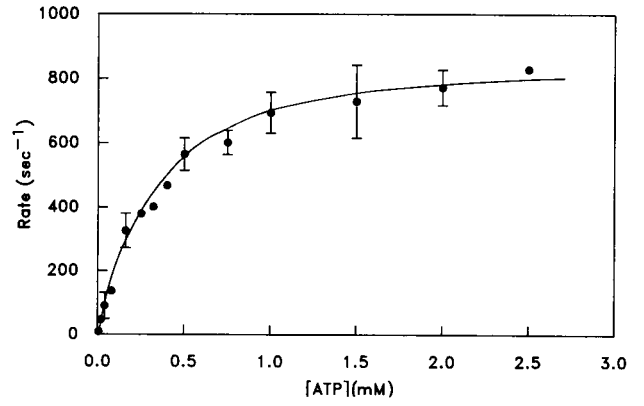

FIGURE 2 Dependence of the apparent rate constant for the binding of ATP to myofibrils on ATP concentration. Points were obtained by fitting the fluorescence transient to a single exponential term as illustrated in Fig. 1. The curve is the fit to an hyperbola, initial slope 3×10^6 M^{-1} s^{-1}, maximum rate 830 s^{-1}. Conditions as for Fig. 1.

TABLE 1 Kinetics of ATP binding to myofibrils and acto-S-1

Conditions	k^a (M^{-1} s^{-1} × 10^{-6})	k_2 (s^{-1})	$1/K_1$ (μM)
10 mM NaCl	4.0	740	200
50 mM NaCl	3.0	830	270
100 mM NaCl	1.9	790	390
150 mM NaCl	1.1	860	620
50 mM NaCl			
20°C	3.0	830	270
10°C	1.0	660	610
5°C	0.6	590	1270
Acto-S-1			
50 mM NaCl			
20°C	2.7	1170	320
10°C	1.4	770	460
5°C	0.9	540	530
50 mM NaCl, methylanthranyloyl ATP	3.0		

Other conditions, 25 mM PIPES, pH 7.0, 2 mM $MgCl_2$, 1 mM EGTA, temperature 20°C except where indicated. Myofibrils and actin are labeled with pyrene (for details see text). Rate constants were fitted to the hyperbolic scheme, $K_1k_2[ATP]/(K_1[ATP] + 1)$ and k^a is the apparent second-order rate constant, $k^a = K_1k_2$,

$$AM + ATP \overset{K_1}{\rightleftharpoons} AM(ATP) \underset{k_{-2}}{\overset{k_2}{\rightleftharpoons}} AM \cdot ATP^*$$

where * indicates a state of enhanced fluorescence of actin in the case of pyrene-labeled proteins or of bound methylanthranyoyl ATP. The maximum rate is taken to be k_2. Similar rate constants were obtained in the presence of calcium.

Various experiments were performed which support the close agreement of the myofibril reaction with the reaction in solution. S-1 was added to saturate the free actin sites in myofibrils. The fluorescence change is now dominated by the S-1 component, and the values of k^a and k_2 agreed within 50% with the values for myofibrils alone. Also the value of k^a for the binding of methylanthranyloyl ATP to unlabeled myofibrils was equal to the value for labeled myofibrils. The maximum rate could not be determined because the signal becomes too small at high nucleotide concentrations.

The rate constants were equal in the presence and absence of calcium within the experimental error. Because the first two steps in the reaction are complete in <5 ms at high ATP concentrations, and myofibrils would have contracted <25 nm per half sarcomere in the presence of calcium, the shortening is not expected to have an effect on the rate of the reaction. This conclusion is strengthened by the observation that cross-linking with 1-ethyl-3-(3-dimethylaminopropyl)--carbodiimide to prevent shortening did not alter the values obtained for the rate constants.

The enhancement of fluorescence of acto-S-1 occurs in the transition to the weakly bound state AM·ATP, and the dissociation of this complex in solution experiments did not give any further change in fluorescence (Taylor, 1991). Thus the rate constant k_2 limits the rate of dissociation of myosin heads. The value of k_2 for myofibrils of about 1000 s^{-1} is smaller than the values reported for the rate of dissociation of acto-S-1 in solution measured by light scattering (Johnson and Taylor, 1978; Millar and Geeves, 1983). The lower value is not caused by labeling of the actin. Measurements of the

rate of dissociation of normal and pyrene-labeled acto-S-1 gave values of 1800–2000 s^{-1} by light scattering. Any difference in the rate constant is within the error of 10–20% in the extrapolated value. However, the rate constant obtained from pyrene fluorescence was 1200 ± 100 s^{-1}. Apparently light scattering gives a larger rate constant than pyrene fluorescence with the same sample under the same conditions (50–100 mM NaCl or KCl, pH 7.0, 20°C).

It is concluded that the rate constant k_2 for myosin heads in myofibrils is essentially the same as acto-S-1 in solution. It is reasonable to assume that the formation of the AM · ATP state in the myofibril is rate limiting for dissociation, and therefore the effective rate of dissociation is at least a 1000 s^{-1} at 20°C. The actual rate of dissociation of the M · ATP state could be 5,000–10,000 s^{-1} based on the dependence of stiffness on the velocity of stretch (Schoenberg, 1988).

The equilibrium constant K_1 for the initial ATP binding step decreased with ionic strength, as would be expected for a charged substrate. This has been discussed previously for acto-S-1 (Johnson and Taylor, 1978). The rate of the isomerization (step 2) is independent of ionic strength but increases with increasing temperature. At physiological temperature, it would be ~2000 s^{-1}.

Phosphate burst and steady-state rate of ATP hydrolysis

The transient or burst phase and the steady-state phase of hydrolysis are shown in Fig. 3 for psoas myofibrils in the absence (*A*) and the presence (*B*) of Ca (10 mM NaCl, 20°C). The size of the burst, as defined by the intercept of the straight line on the vertical axis, is close to one for relaxed myofibrils. In the presence of Ca the transient rate is much larger and the burst is small. The steady-state rate is large, ~20 s^{-1}. This value applies to the brief period of 100 ms. At longer times the myofibrils have contracted to lengths below 2.0 μm and some show contraction bands. The steady-state rate measured by mixing by hand and stopping the reaction at times ranging from 5 to 15 s is about three times smaller and applies to supercontracted myofibrils.

Synthetic thick filaments probably provide the best reference state for the hydrolysis reaction of dissociated myosin heads. In myofibrils at low ionic strength in the relaxed state, an appreciable fraction of the cross-bridges are expected to be bound to actin (Schoenberg, 1988; Yu and Brenner, 1989), which could affect the rate constant of the hydrolysis step. Rate constants for thick filaments and relaxed and active myofibrils are given in Table 2. For relaxed myofibrils the transient rate is smaller but the burst size is larger than for thick filaments. However, the possible error in the estimation of the myosin site concentration of myofibrils could account for much of the difference in burst size.

The rate constant for the phosphate burst transient in the active state is much larger than in the relaxed state, and it was difficult to measure accurately at 20°C. Data at 10°C are included in Table 2 as well as data for back muscle myofibrils at a higher ionic strength.

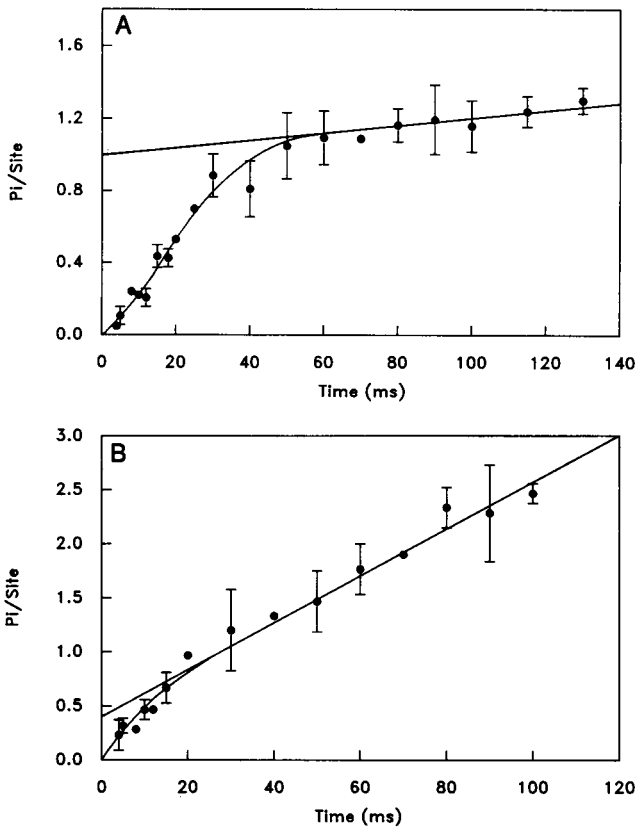

FIGURE 3 Transient and early steady-state hydrolysis of ATP by psoas myofibrils. (*A*) Relaxed myofibrils, conditions as for Fig. 1 except salt concentration is 10 mM, 2 mg/ml myofibrils, 100 μM MgATP. Error bars refer to range of duplicate or triplicate determinations. Transient rate constant 50 s^{-1}, steady-state rate 1.8 s^{-1}, burst 1 mol/mol of sites. (*B*) Activated myofibrils, conditions as for *A*, except EGTA replaced by 0.5 mM $CaCl_2$. Transient rate constant is ~150 s^{-1}, steady-state rate 20 s^{-1}, burst 0.4 mol/site.

Because it was shown that the rate constants for the ATP binding and dissociation steps are large, the transient phase of phosphate formation shows only a very short lag. The transient and steady-state phases can be represented by adding two steps to the mechanism and treating the association and dissociation steps for substrate and product intermediates as equilibria. The kinetic mechanism is

$$E \cdot ATP \underset{\bar{k}_{-3}}{\overset{\bar{k}_3}{\rightleftharpoons}} E \cdot ADP \cdot P \overset{\bar{k}_e}{\rightleftharpoons} E + ADP + P \qquad (2)$$

where E is the sum of associated and dissociated states in equilibrium and bars indicate average rate constants (see section on Analysis of Kinetics).

The three rate constants $\bar{k}_3$, $\bar{k}_{-3}$, and $\bar{k}_e$ are calculated from the three observed quantities, the transient rate constant λ, the burst *B*, and the steady-state rate *V* (Table 2).

The salient points are that the rate constant $\bar{k}_3$ is approximately the same for thick filaments and active myofibrils, and the effective rate constant of product release is smaller than the rate of the hydrolysis step. The rate constant for the hydrolysis step is smaller for relaxed myofibrils as compared with thick filaments.

TABLE 2 Kinetics of ATP hydrolysis by myofibrils and thick filaments

Conditions	Transient rate ($\lambda(s^{-1})$)	Burst per site B	Steady state $V(s^{-1})$	Calculated rate constants (s^{-1})		
				$\bar{k}_3$	$\bar{k}_{-3}$	$\bar{k}_e$
Psoas, 20°C						
Thick filaments	85	0.7	0.12	60	25	0.17
Myo, −Ca	60 ± 10	1 ± 0.1	1.5 ± 0.3	60	5	1.5
Myo, +Ca	140 ± 15	0.35 ± 0.1	22 ± 2	70 ± 5	25 ± 5	40 ± 5
Psoas, 10°C						
Thick filaments	40	0.6	0.03	24	16	0.05
Myo, −Ca	21	0.8	0.12	17	4	0.15
Myo, +Ca	55	0.3	6.5	23	17	15
Back, 20°C						
Thick filaments	75	0.65	0.1	49	26	0.15
Myo, −Ca	45 ± 5	0.8	0.5	37 ± 4	8 ± 1	0.6
Myo, +Ca	80 ± 10	0.3 ± .05	12 ± 2	36 ± 5	17 ±	27 ± 5

Other conditions: pH 7, 10 mM NaCl for psoas, 40 mM NaCl for back muscle, 1 mM EGTA or 0.5 mM $CaCl_2$ for −Ca and +Ca, respectively. Rate constants calculated for the scheme

$$E \cdot ATP \underset{\bar{k}_{-3}}{\overset{\bar{k}_3}{\rightleftharpoons}} E \cdot ADP \cdot P \overset{\bar{k}_e}{\rightleftharpoons} E + ADP + P$$

where E is the sum of associated and dissociated states in rapid equilibrium.

The kinetic parameters λ, B, and V for back muscle myofibrils were measured at 10 mM and 40 mM NaCl and extrapolated to zero added salt. The values agreed with our values for acto-S-1 and regulated acto-S-1 prepared from back muscle (Rosenfeld and Taylor, 1987; Rosenfeld and Taylor, 1984a). In comparing the values it is assumed that the fractional association is 0.5–0.6 for myofibrils (Schoenberg, 1988; Yu and Brenner, 1989). It was also observed previously (Rosenfeld and Taylor, 1987) for regulated acto-S-1 that the transient rate λ is smaller in the relaxed state compared with S-1 (30 s^{-1} vs. 43 s^{-1}, respectively), while the corresponding values for myofibrils are 25 s^{-1} and 40 s^{-1}. The burst size and therefore the equilibrium constant was the same for S-1 and acto-S-1 and, in this case, site concentration is not a source of error. Therefore the rate of the hydrolysis step is reduced by the interaction with actin in the relaxed state even though the AM·ATP state is weakly bound. The same conclusion appears to hold for relaxed myofibrils, but errors are larger because of uncertainty in myosin head concentration.

The rate of product release $\bar{k}_e$ is 40–100 times smaller for relaxed versus active myofibrils. In 10 mM NaCl an appreciable fraction of myosin heads should be bound as AM · ATP and AM · D·P states. Therefore regulation by Ca at low ionic strength must include inhibition of a step in product release as well as a possible reduction in the binding constant of the weakly bound states.

The effect of ionic strength on rate constants was investigated. It has been shown previously that the rate constant of the hydrolysis step increases with ionic strength based on measurements of phosphate formation or tryptophan fluorescence, and there was also a small increase in the size of the phosphate burst (Johnson and Taylor, 1978; Rosenfeld and Taylor, 1984a). The same trend was observed for thick filaments. The rate constant increased from 50–60 s^{-1} in 10 mM NaCl to 100–110 s^{-1} in 100 mM, and the burst increased from 0.6 to 0.9 for back muscle thick filaments. Transient state rate constants are plotted in Fig. 4 for psoas thick filaments and myofibrils. The rate constant for relaxed myofibrils more than doubled with ionic strength and became approximately equal to the rate constant for thick filaments at 100 mM salt. The phosphate burst size was one for thick filaments and 1.1 ± 0.1 for relaxed myofibrils. The results indicate that at high ionic strength the kinetic behavior of cross-bridges corresponds to a dissociated state, while at low ionic strength there is appreciable binding and the rate constant for hydrolysis is smaller for the attached cross-bridge. In the active state there is little change in the transient rate constant with ionic strength and there is a decrease in the difference between rate constants for active and relaxed

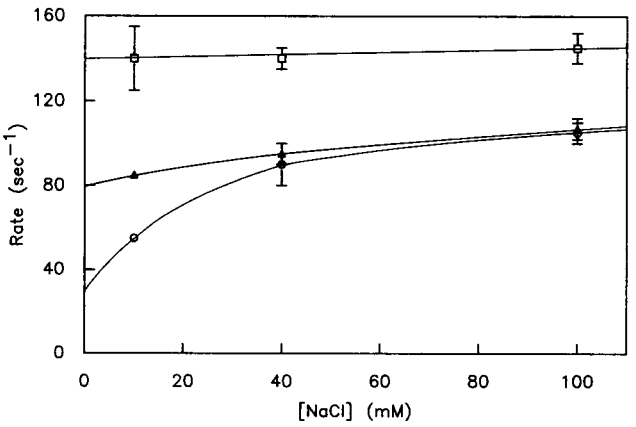

FIGURE 4 Dependence of rate of transient hydrolysis phase on salt concentration for psoas myofibrils and thick filaments. Ionic strength was varied with NaCl, buffer conditions as in Fig. 1, relaxed myofibrils contained 1 mM EGTA, active myofibrils contained 0.5 mM $CaCl_2$. △: thick filaments; ○: relaxed myofibrils; □: active myofibrils.

states. The phosphate burst increased to a value close to 1 in the active state. A similar trend was observed for back muscle myofibrils (data not shown).

The steady-state rate was nearly independent of ionic strength from 10 to 100 mM salt, 22 s^{-1} for psoas and 12 s^{-1} for back myofibrils. As described in a later section, the velocity of shortening was also not dependent on ionic strength.

Individual rate constants could not be calculated accurately from the data at high ionic strength. Since the burst is large, $\bar{k}_3$ must be much larger than $\bar{k}_e$, and $\bar{k}_e$ has to be larger than the steady-state rate. Thus $\bar{k}_e$ is 25–30 s^{-1}, $\bar{k}_3$ is 130–140 s^{-1}, and $\bar{k}_{-3}$ is small. Thus at high ionic strength the effective rate of product release is rate limiting, while for acto-S-1 at low ionic strength and very high actin concentration the hydrolysis step is rate limiting. The significance of the difference in rate-limiting step will be considered in the Discussion section.

Inhibition by ADP and phosphate

ADP is expected to be a competitive inhibitor of ATP binding. The inhibition was investigated by measuring the transient rate constant of ATP binding for a range of ADP concentrations using the change in fluorescence of pyrene-labeled myofibrils. The time course of the fluorescence change fitted a single exponential term, and the rate constant fitted a hyperbolic dependence on ATP concentration. A double reciprocal plot of rate constant versus ATP concentration is shown in Fig. 5 for a range of ADP concentrations.

We first consider the case that ADP is in rapid equilibrium with actomyosin sites in the myofibril (see section on Analysis of Kinetics). The apparent second-order rate constant of ATP binding in the presence of ADP is $k^a/(1 + [ADP]/K_D)$,

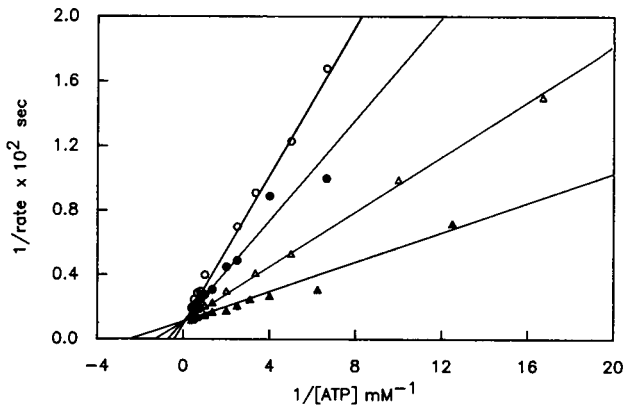

FIGURE 5 The dependence of the rate of ATP binding to myofibrils on the concentration of ADP. The reciprocal of the rate constant of ATP binding is plotted against the reciprocal of the ATP concentration for ADP concentrations of 0 (▲), 50 μM (△), 150 μM (●), and 250 μM (○). Conditions, 20°C, 25 mM PIPES buffer, pH 7.0, 50 mM NaCl, 2 mM $MgCl_2$, 0.5 mM $CaCl_2$, 0.4 mg/ml myofibrils, concentrations of Mg ATP and column-purified Mg ADP as indicated. Myofibrils also contained P^1,P^5-di[adenosine-5'] pentaphosphate to prevent contraction in presence of ADP.

where K_D is the dissociation constant of ADP. Since this expression is the slope of the double reciprocal plot, K_D was determined from a secondary plot of slopes versus ADP concentration. The value is 0.1 mM. This value is in the range reported for equilibrium binding measurements of ADP to acto-S-1 and myofibrils (Biosca et al., 1986; Sleep and Glyn, 1986) and kinetic studies of ADP dissociation from acto-S-1 (Taylor, 1991).

There are at least two ADP states in the acto-S-1 kinetic scheme (Sleep and Hutton, 1980; Taylor, 1991). What is the significance of the dissociation constant calculated from the inhibition experiments, and is it valid to assume that ADP is in rapid equilibrium? There are at least three steps in product dissociation which up to this point has been represented by a single effective rate constant $\bar{k}_e$, whose value is determined by the rate constants of these steps:

$$AM \cdot D \cdot P \overset{k_{4(-P)}}{\rightleftharpoons} AM' \cdot D \overset{k_5}{\rightleftharpoons} AM(D) \overset{k_6}{\rightleftharpoons} AM + D.$$

Step 6 is a rapid equilibrium step based on studies of acto-S-1 in solution (Taylor, 1991). If the AM'·D state is present in appreciable amounts at equilibrium with ADP, the rate of ATP binding would be affected by k_5. The time course of the binding of ATP would then fit two exponential terms with rate constants k_5 and $K_1k_2/(1 + K_1[ATP] + [ADP]/K_6)$. At very high ATP concentrations, the rate constants are k_5 and k_2. The data fitted a single exponential term which is not consistent with this mechanism. In solution, k_5 is 300–400 s^{-1} (Taylor, 1991), and if this value is approximately correct for myofibrils, the deviation of the fit from a single exponential would be evident only at very high ATP concentrations. However, step 5 has a large temperature dependence, and to determine whether this step could be limiting, the rate of ATP binding a set of measurements was made at 5°C for myofibrils and acto-S-1. The effective rate of ADP dissociation (k_5) for acto-S-1 was measured by mixing the S-1-ADP complex with pyrene-labeled actin, and a value of 10–20 s^{-1} was obtained, which agrees with our previous results (Taylor, 1991). The rate of ATP binding to myofibrils or acto-S-1 at 5°C fitted a hyperbola with maximum rate >100 s^{-1} for a range of ADP concentrations up to 0.2 mM. Thus the results indicate that step 5 does not limit the rate of ADP dissociation. This conclusion is consistent with a large value of K_5 (at least 10) so that in the equilibrium mixture only the AM(D) state is present and the dissociation constant measured in the experiment is K_6.

The addition of 20 mM phosphate alone or in addition to ADP did not change the rate constant of ATP binding after adjusting for the increase in ionic strength. Also, the addition of up to 100 mM phosphate did not inhibit the steady-state rate of hydrolysis of ATP. Phosphate appears to be too weakly bound to AM or AM(D) to influence the distribution of intermediate states.

Velocity of shortening

The velocity of shortening of prestretched myofibrils was measured by mixing with ATP and stopping the reaction by

mixing with acetate buffer at pH 4.5 using the quench flow apparatus. Control experiments in which the order of mixing was reversed showed that the pH jump stopped shortening in <10 ms. However, there is a range of initial lengths in the preparation; consequently, the standard error in length measurements is relatively large. At high ionic strength, 100 mM NaCl, and 1 mM ATP, the velocity was constant over the range of shortening from 2.6 to 2.0 μm, with a value of 6 μm s^{-1} per half sarcomere at 20°C (Fig. 6).

It is necessary to determine the dependence of the velocity of shortening on ATP concentration (the K_M for shortening). At 100 μM ATP the velocity was approximately 2.5 μm s^{-1} (Fig. 6), which corresponds to a K_M of ~150 mM. However, for times longer than 30 ms, the velocity decreased to one-half to one-third of the initial value and remained nearly constant up to times of 100–150 ms.

Measurements at lower ionic strengths showed the same effect. The initial velocity in 1 mM ATP was 5–6 μm s^{-1} in 40 mM and 10 mM NaCl, but the velocity decreased after 30 ms.

The explanation of a nonlinear velocity of shortening is not clear. A similar result was obtained by Ohno and Kodama (1991) in their studies in which the quench flow technique was introduced. Gulati and Podolsky (1981) also reported a small curvature in velocity plots at low ionic strength.

It is concluded that the K_M for shortening is in the range of 100–200 μM, but the quench flow method was not suitable for an accurate measurement.

DISCUSSION

The data on myofibril kinetics are adequately represented by the kinetic scheme derived from studies of actomyosin in solution. The scheme expanded to include the phosphate dissociation step deduced mainly from fibers (Hibberd et al., 1985; Millar and Homsher, 1990; Dantzig et al., 1992) is

$$\underset{}{\overset{(1)}{}} \quad \overset{(2)}{} \quad \overset{(3)}{}$$
$$AM + T \rightleftharpoons AM(T) \rightleftharpoons AM \cdot T \rightleftharpoons AM \cdot D \cdot P$$
$$\overset{(4)}{} \quad \overset{\text{fast}}{} \quad \overset{(5)}{} \quad \overset{(6)}{}$$
$$\rightleftharpoons AM' \cdot D \cdot P \underset{(-P)}{\longrightarrow} AM' \cdot D \rightleftharpoons AM(D) \rightleftharpoons AM + D.$$

Scheme 1

The constants K_1, k_2, $\bar{k}_3$, $\bar{k}_{-3}$, and K_6 were determined from the experimental data. It is assumed in accord with Dantzig et al. (1992) that the phosphate dissociation step is a rapid equilibrium. The experiments on inhibition of ATP binding by ADP are consistent with a rapid equilibrium for step 6 and a relatively large value for the equilibrium constant K_5. In this case the effective rate constant for dissociation of products and completion of the cycle, $\bar{k}_e$ is given by $\bar{k}_e = \bar{k}_4 k_5/(k_4 + k_5)$. A bar is omitted for k_5, since it is assumed that the AM'·D is not in rapid equilibrium and that the fractional dissociation is small. The rate constant k_5 could not determined directly for myofibrils; the value of this rate constant is important, since this step probably determines the maximum velocity of shortening (Siemankowski et al., 1985).

The value of k_5 was determined from K_M, the dependence of the velocity of shortening on ATP concentration. The expression for K_M in terms of the measured rate constants is $K_M = k_5/k^a(1 + k_5/k_2)$ using the simple model described in the Analysis of Kinetics section. The value of K_M is ~150 μM based on myofibril shortening measurements (100 mM NaCl, 20°C). Because of curvature in velocity plots, the value could not be measured satisfactorily at lower ionic strength. Values of K_M for psoas fibers (150 μM at 10°C and 200 mM ionic strength (Pate and Cooke, 1989a)) and actin filaments (88 μM at 25°C and 50 mM salt (Homsher et al., 1992), 180 μM at 22°C and 100 mM salt (Harada et al., 1990)) are in the same range.

The value of k_5 is 400–450 s^{-1}at 20°C and 100 mM salt based on our data and ~400 s^{-1} in 50 mM salt using the K_M value of Homsher et al. (1992). Because k_5 is an order of magnitude larger than k_e, the effective rate of product dissociation is determined by k_4, which is ~10% larger than k_e.

Thus a set of rate constants or equilibrium constants for the steps in rapid equilibrium can be assigned for the six-step kinetic scheme for myofibrils. It is concluded that the values of the constants for myofibrils undergoing unloaded shortening are very similar to the values for acto-S-1 in solution. The rate constants for ATP binding and isomerization could be compared over a range of ionic strengths and temperatures and the values agree within a factor of 2. The value of k^a agreed with measurements using tryptophan fluorescence (White, 1985) and ATP chase experiments (Herrmann et al., 1992; Houadjeto et al., 1992). However, the value of k^a is at the high end of the range reported for fibers using photolysis of caged ATP (Goldman et al., 1984). The values for the

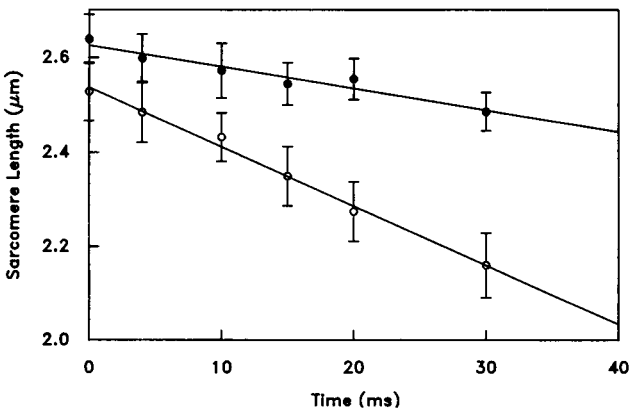

FIGURE 6 Time course of myofibril contraction. Contraction was initiated by mixing psoas muscle myofibrils with Mg ATP in the quench flow apparatus. Contraction was stopped by mixing with 0.4 M sodium acetate buffer, pH 4.5. Error bars represent range of 30 measurements of sarcomere lengths. Conditions as for Fig. 5 except the buffer contained 100 mM NaCl. The velocity is 6 μm/s per half sarcomere in 1 mM MgATP (○) and 2.5 μm/s in 100 μM MgATP (●).

transient phase of the hydrolysis step and the effective rate of product release could only be compared at low ionic strength. The values are in agreement, assuming that the association of substrate and product states is 0.5–0.6.

The value of k_5, the rate constant for isomerization of the AM′·D state, was previously measured for back muscle acto-S-1 at low ionic strength using etheno-ADP, which gave a value of 275–350 s^{-1} (Rosenfeld and Taylor, 1987) or the fluorescence of pyrene-labeled actin, which gave only 160 s^{-1} (Taylor, 1991). It was suggested that labeling the actin may have reduced the value. The value was redetermined using methylanthranyloyl ADP using the same method as in previous studies. The complex of S-1 with methylanthranyloyl ADP was reacted with actin plus ATP, and the observed rate constant was extrapolated to infinite actin concentration to obtain k_5. A value of 325 ± 25 s^{-1} was obtained in 10 mM NaCl at 20°C. The value decreased to 225 s^{-1} in 25 mM NaCl, and it is probably <200 s^{-1} in 50 mM NaCl, but the extrapolation is not accurate because the binding of the S-1 nucleotide complex is too weak (data not shown). Therefore k_5 measured in solution appears to be smaller by a factor of 2 compared with the value calculated for myofibrils. In view of the uncertainties from the use of labeled proteins or substrate analogues in solution measurements and the error in K_M for myofibrils, the difference may not be significant, but the rate constant for myofibrils appears to be at least as large and probably larger than in solution. The value of K_6 is in reasonable agreement with the value obtained from the reduction of shortening velocity of fibers by ADP (Cooke and Pate, 1985), which strengthens the interpretation that velocity is determined by the time to complete the cycle from the AM′ · D state.

The results are in partial agreement with other recent studies on myofibrils. A phosphate burst close to 1 has been reported for myofibrils and fibers (White, 1985; Ohno and Kodama, 1991; Ferenczi, 1986; Ferenczi et al., 1984). The most extensive studies on myofibrils by Barman and Travers and their collaborators (Houadjeto et al., 1992; Herrman et al., 1992) were done at high ionic strength and low temperature, which makes a direct comparison difficult. In one series of experiments at 15°C and low ionic strength, our results agree that the phosphate burst is small, although our rate constants for the transient and steady state are larger. These authors also concluded that the equilibrium constant for the hydrolysis step is large in the presence or absence of Ca at high ionic strength.

The kinetic scheme and the mechanism of shortening

The quantitative interpretation of the ATPase cycle in muscle fibers has been based on the kinetic behavior of acto-S-1 at very low ionic strength and very high actin concentration. Under these conditions, the phosphate burst is small, the fractional association of substrate and product states is large, hydrolysis is the rate-limiting step ($k_3 < k_c$), and an appreciable fraction of the hydrolysis occurs via the AM · T state, which is the predominant intermediate (Rosenfeld and Taylor, 1984). Myofibril data extrapolated to low ionic strength agreed with acto-S-1 data, except that the fractional association of substrate and product states probably does not exceed 0.5–0.6 and $\bar{k}_3$ is comparable to $\bar{k}_c$. On the contrary, the results for myofibrils at high ionic strength showed that product release is the rate-limiting step. It is important to consider the implications of the kinetic scheme under more nearly physiological conditions.

The effects of increasing the ionic strength are to increase the rate of the hydrolysis step, to increase the equilibrium constant for hydrolysis as measured by the size of the phosphate burst, and to reduce $\bar{k}_c$. The fractional association of substrate and product states is known to decrease with increasing ionic strength in solution, and the same effect is expected in myofibrils and fibers. This decrease is indicated by the trend in the rate constants for the transient hydrolysis phase shown in Fig. 5. The difference in rate constants for active and relaxed states is smaller and the value for the relaxed state is equal to the fully dissociated state as measured for thick filaments. The smaller value of $\bar{k}_c$ is consistent with a lower association, since $\bar{k}_c$ is proportional to the fractional association of the AM′ · ADP state.

The values of the rate constants cannot be calculated accurately from the data at high ionic strength, but to illustrate the properties of the system, we consider a set of rate constants which are consistent with the observations. It is assumed that the fractional binding of M · ATP and M · ADP · P is reduced at least twofold at 100 mM salt compared with 10 mM salt to a value of 0.2–0.25 at 20°C. The data fits values of $\bar{k}_c$ of 25–30 s^{-1}, $\bar{k}_3$ of 140 to 150 s^{-1}, and $\bar{k}_{-3}$ small. A set of rate constants for the scheme is;

$$\begin{array}{ccccc} & \geq 1000\ s^{-1} & & \leq 150\ s^{-1} & \\ AM & \longleftrightarrow & AM \cdot T & \longleftrightarrow & AM \cdot D \cdot P \\ & (+T) & \updownarrow & & \updownarrow \\ & & & 150\ s^{-1} & \\ & & M \cdot T & \longleftrightarrow & M \cdot D \cdot P \\ & & & <15\ s^{-1} & \end{array}$$

$$\begin{array}{ccccccc} & 140\ s^{-1} & & \text{fast} & & 500\ s^{-1} & \\ \longleftrightarrow & AM' \cdot D \cdot P & \longleftrightarrow & AM' \cdot D & \longleftrightarrow & AM + D. \\ & & & (-P) & & & \end{array}$$

A value of 28 s^{-1} for $\bar{k}_c$ gives 30 s^{-1} for $\bar{k}_4$. A fractional association of AM · ADP · P of 0.22 gives 30/0.22 = 140 s^{-1} for k_4. This set of constants gives a steady-state rate V of 23 s^{-1}, a transient rate constant for the burst of 178 s^{-1}, and a burst size of 0.7. The measured burst was closer to 1, but the value may have been overestimated because of an error in myosin site concentration. The distribution of intermediates in the steady state is AM = 0.027, AM · ATP plus M · ATP = 0.17, AM · ADP · P + M · ADP · P = 0.74, AM′ · ADP = 0.047. The main bound state is AM · ADP · P (0.15–0.2 depending on the

degree of association) and the predominant pathway is detachment, hydrolysis, and reattachment followed by the steps in product release as was proposed in an earlier model (Lymn and Taylor, 1971).

The kinetic scheme can account for some properties of myofibrils and fibers, but the limitations of this simple treatment need to be considered. The steady-state ATPase is given by $V = \bar{k}_3\bar{k}_e/(\bar{k}_3 + \bar{k}_{-3} + \bar{k}_e)$. It was found that V is not very dependent on ionic strength. The decrease in $\bar{k}_e$ with increase in ionic strength caused by a decrease in association of the M·ADP·P state is compensated by the increase in rate and equilibrium constant of the hydrolysis step. The velocity of shortening $U = dk_5/(1 + k_5/k_2)$ where d is the step size. k_5 has a Q_{10} of 2.5 based on solution measurements, which accounts for the dependence of shortening velocity on temperature. However, k_5 increases with decreasing ionic strength, while the velocity of fibers and actin filaments decreases for ionic strengths below 50–75 mM (Gulati and Podolsky, 1981; Homsher et al., 1992). The simple model neglected the drag of AM·ATP and AM·ADP·P states which may be significant at low ionic strength (Tawada and Sekimoto, 1991). The scheme does not predict a correlation between V and U because V is determined primarily by $\bar{k}_4$ and U by k_5. The relation between U and V can also be expressed as $U/V = d/r$, where r is the duty cycle ratio which is the fraction of the cycle time during which the cross-bridge exerts a force. Kinetic data on different muscle types is needed to determine whether the duty cycle ratio is constant.

An objection could be raised to the interpretation of the kinetic scheme on the basis of stiffness measurements. In fibers undergoing unloaded shortening the stiffness relative to the isometric stiffness is 0.1–0.3 (Brenner, 1988; Griffith et al., 1993). The relative stiffness is usually interpreted as the fraction of cross-bridges which can maintain a force and therefore are strongly bound. In the kinetic scheme the fraction of the myosin heads which contribute to force is $V\tau$, which is approximately 20/400 = 0.05. However, if the stiffness is the same if one or both heads are strongly attached and the relative stiffness is as large as 0.2, the fraction of strongly attached heads is only 0.1. Also some recent evidence suggests that weakly attached states may contribute to stiffness (Stehle et al., 1993). Thus the kinetic scheme need not be in contradiction with stiffness measurements.

The current interpretation of the contraction mechanism is that the transition from AM · ADP · P to AM′ · ADP plus phosphate introduces a strain d in the cross-bridge which generates a force and the increase in the strain free energy is expected to reduce the rate constant of the transition in which force is developed. However, there was no significant reduction in rate constants for shortening myofibrils compared to acto-S-1.

The rate constant k_4 is the frequency of the transition from a weakly attached state which is expected to have a small or nearly zero strain to the strained AM′ · D state (or AM′ · D · P). The transition itself can be regarded as instantaneous relative to the motion and it should experience the same effect of strain as in an isometric contraction. In any case, the rate constant k_4 has been measured for the isometric case by several methods which give values of 50 to 100 s^{-1} (Goldman et al., 1984; Dantzig et al., 1992; Brenner and Eisenberg, 1986; Kawai and Halvorson, 1989) which are within a factor of 2 of the value for myofibrils. Theoretical models are also consistent with reduction of the forward rate constant of this step by strain (Dantzig et al., 1992; Pate and Cooke, 1989).

It is possible but unlikely that the step in which force is developed is an additional fast step in the mechanism and k_4 is a slower step which follows it. A small effect of strain on the rate of step 4 might be explained if the strain energy is small for this step. If the strain is only 4 nm which is the size of the release which reduces isometric force to 0 and the force per bridge is 2 pN, then the stiffness is 5×10^{-4} Nm^{-1}. In this case the strain energy is only k_bT which would reduce k_e by e^{-1} or a factor of 2.7 if the effect is on the forward rate constant and a factor of 1.6 if the effect is equally distributed between the forward and reverse steps. A factor of 2 is within the accuracy of the comparison of solution and myofibril data, since the degree of association is uncertain.

A large effect of tension on rate constants has to be invoked to explain the difference in V for isometric versus unloaded shortening. The value is 20 s^{-1} for myofibrils in this work and ~2–3 s^{-1} for isometric psoas fibers at 20°C (Ferenczi et al., 1984; Glyn and Sleep, 1985). White et al. (1993) reported similar rates for isometric fibers and acto-S-1 at 10°C which appears to contradict our interpretation, unless there is a change in rate-limiting step at lower temperature. Although lower values have also been reported for myofibrils (Houadjeto et al., 1992), a value of 14 s^{-1} at 22°C can be calculated from Fig. 4 of Harada et al. (1990). The rate constant of the burst remains high (Ferenczi, 1986) and k_4 is also large based on the rate of tension redevelopment. Therefore, to reduce V to 4 s^{-1} requires k_5 to be reduced to ~5 s^{-1}. Since the kinetic scheme requires k_5 to be 400–500 s^{-1} to account for unloaded shortening, the reduction is 100-fold. This might be explained by a further rotation (distortion) of the bridge in step 5. An increase in strain energy of 4.6 k_bT is required to reduce the rate constant by 100-fold, which corresponds to an additional strain of 6 nm for a total of 10 nm for both transitions. Huxley and Simmons (1971) proposed multiple transitions between force-generating states to explain force transients. A similar explanation could account for the effects of tension on rate constants of the kinetic scheme.

The consequence of making k_5 the rate-limiting step for the cycle is that AM′·D is the main intermediate state. In solution studies AM′·D is more strongly bound than the substrate and the first product states, but the binding constant may be only increased by a factor of 10 (Rosenfeld and Taylor, 1987; Taylor, 1991). This is sufficient to give a large increase in binding of bridges in the isometric state compared to unloaded shortening. The rate of detachment of bridges in the AM′·D state is still fairly large compared to the rigor state

which is consistent with the proposal of Brenner (1991) that a force-generating state can detach and reattach.

The kinetic scheme and the step size problem

The step size d can be calculated from the rate constants k^a, k_2, and k_5 and the velocity of shortening using the simple model of the cycle given in the section on Analysis of Kinetics; $U = d/\tau$, where $1/\tau = k_5/(1 + k_5/k_2) = K_M k^a$. The value of d is 19 nm at 20°C and 100 mM NaCl (k_5 = 450 s^{-1}, k_2 = 1000 s^{-1}). We have previously reported a value of 20 nm based on preliminary data on myofibril kinetics (Taylor, 1989). The simple model omits the lag in the decay of force, and the value is 15 nm calculated from the two-step model. The value is somewhat larger than 10–12 nm figure of the conventional model, but the difference is within the uncertainty in the values of the rate constants.

This value of d is larger than obtained by Pate et al. (1993a,b) and White et al. (1993) who used essentially the same kinetic method. Their values ranged from 4.6 to 7.1 nm for ATP and other nucleotide triphosphates. White et al. (1993) obtained 4.6 nm for d from the relation $U = dK_M k^a$ using a value of k^a of 2.7 × 10^6 M^{-1} s^{-1} at 10°C and 200 mM ionic strength based on light scattering data for acto-S-1 in solution. We obtained 1.1 × 10^6 M^{-1} s^{-1} for k^a by light scattering under the same conditions (Johnson and Taylor, 1978) and 0.6 × $10^6 M^{-1}$ s^{-1} from myofibrils using pyrene fluorescence. As already noted, light scattering measurements tend to give a larger rate constant than fluorescence measurements made on the same sample.

Pate et al. (1993b) used the same kinetic data but calculated d from a model in which the force-generating state decays only in the region of negative strain as in the Huxley (1957) model. This assumption increases the calculated value of d by a factor of $\sqrt{2}$. In the present work we have used rate constants obtained from myofibrils and we assume that effects of strain have already been taken into account in the measured values.

In view of the disagreements in values of kinetic constants and the influence of the details of the model on the calculation, it is concluded that d is in the range 10 ± 5 nm but the value is not known accurately.

The problem is to explain why there is such a large variation in the values obtained for the "step distance" (reviewed by Burton (1992). The values range from 10 to 20 nm (motility assay, spectrum of movement steps) (Uyeda et al., 1990, 1991) to >40 nm (distance versus ATP hydrolysis in skinned fibers (Higuchi and Goldman, 1991) to >100 nm from the work of Yanagida and collaborators (motility assays including myofibrils, damping of force fluctuations) (Harada et al., 1990; Ishijima et al., 1991).

All the experiments based on motility assays use the same simple model that was used in the present work, $U = dV/r$. U/V is measured and d is obtained from an estimate of r.

The value of U/V in this paper is 300–400 nm, while Harada et al. (1990) obtained a value only 60% larger (not corrected for turnover rate in the absence of Ca) and Higuchi and Goldman (1991) actually give a value two times smaller (in their case it is the ratio of distance to amount of hydrolysis). The large difference in the values of d must be due primarily to different estimates of r. In addition, there is uncertainty in the choice of the appropriate value of the cycle rate to use in motility assays in which the interaction is not a complete cycle. This problem does not arise in myofibril assays at high ionic strength. The value of r obtained from kinetics is ~0.05. This value agrees with the value of Uyeda et al. (1990) who obtained 10–20 nm for d. Higuchi and Goldman use r equal to 0.4 based on stiffness, while Yanagida and collaborators use an r value close to 1 based on their interpretation of kinetics and on the interpretation of force fluctuations.

It is evident that most of the disagreement is in the interpretation of models from which the duration of force-generating states is calculated. The answer from transient kinetics also depends on a model, but it was shown that the kinetic model accounts for a body of evidence on the properties of myofibrils and it leads to a step distance in agreement with the conventional interpretation of the cross-bridge cycle.

We thank Aldona Rukuiza for technical assistance, and Camille Steber, who did the initial experiments with labeled myofibrils. This work was supported by National Institutes of Health L. B. Program Project Grant HL 20592.

REFERENCES

Biosca, J. A., L. E. Greene, and E. Eisenberg. 1986. Binding of ATP and ATP analogues to cross-linked and non-crosslinked acto-S 1. *J. Biol. Chem.* 261:9793–9800.

Brenner, B. 1988. Experimental approach to determine cross-bridge turnover kinetics during isometric and isotonic steady state contraction. *Pfluegers Arch.* 411:R 186.

Brenner, B. 1991. Rapid dissociation and reassociation of actomyosin cross-bridges during force generation. *Proc. Natl. Acad. Sci. USA.* 88: 10490–10494.

Brenner, B., and E. Eisenberg. 1986. Rate of force generation in muscle: correlation with actomyosin ATPase activity in solution. *Proc. Natl. Acad. Sci. USA.* 83:3542–3546.

Burton, K. 1992. Myosin step size: estimates from motility assays and shortening muscle. *J. Muscle Res. Cell Motil.* 13:590–607.

Cooke, R., and E. Pate. 1985. Effects of ADP and phosphate on the contraction of muscle fibers. *Biophys. J.* 48:789–798.

Dantzig, J. A., Y. E. Goldman, N. C. Millar, J. Lactis, and E. Homsher. 1992. Reversal of the cross-bridge force generating transition by photogeneration of phosphate in rabbit psoas muscle fibers. *J. Physiol. (Lond.).* 451:247–278.

Duke, J., R. Takashi, K. Ue, and M. F. Morales. 1976. Reciprocal reactivities of specific thiols when actin binds to myosin. *Proc. Natl. Acad. Sci. USA.* 73:302–306.

Ferenczi, M. A. 1986. Phosphate burst in permeable muscle fibers of the rabbit. *Biophys. J.* 50:471–477.

Ferenczi, M. A., E. Homsher, and D. R. Trentham. 1984. Kinetics of magnesium adenosine triphosphate cleavage in skinned muscle fibers of the rabbit. *J. Physiol. (Lond.).* 352:575–599.

Glyn, H., and J. A. Sleep. 1985. Dependence of ATPase activity of rabbit psoas muscle fibers and myofibrils on substrate concentration. *J. Physiol. (Lond.).* 365:259–276.

Goldman, Y. E., M. G. Hibberd, and D. R. Trentham. 1984. Relaxation of rabbit psoas muscle fibers from rigor by photochemical generation of adenosine 5′ triphosphate. *J. Physiol. (Lond.).* 354:577–604

Griffith, P. J., C. C. Ashley, M. A. Bagni, Y. Maeda, and G. Cecchi. 1993. Cross-bridge attachment and stiffness during isotonic shortening of intact single muscle fibers. *Biophys. J.* 64:1150–1160.

Gulati, J., and R. J. Podolsky. 1981. Isotonic contraction of skinned muscle fibers on a slow time base. *J. Gen. Physiol.* 78:233–257.

Harada, Y., K. Sakurada, T. Aoki, D. D. Thomas, and T. Yanagida. 1990. Mechanochemical coupling in actomyosin energy transducion studied by in vitro movement assay. *J. Mol. Biol.* 77:549–568.

Herrmann, C., M. Houadjeto, F. Travers, and T. Barman. 1992. Early steps in the Mg^{2+}-ATPase of relaxed myofibrils. *Biochemistry.* 31:8036–8042.

Hibberd, M. G., J. A. Dantzig, D. R. Trentham, and Y. E. Goldman. 1985. Phosphate release and force generation in skeletal muscle fibers. *Science.* 228:1317–1319.

Hibberd, M. G., and D. R. Trentham. 1986. Relationships between chemical and mechanical events during muscular contraction. *Annu. Rev. Biophys. Chem.* 15:119–161.

Higuchi, H., and Y. E. Goldman. 1991. Sliding distance between actin and myosin filaments per ATP molecule hydrolysed in skinned muscle fibers. *Nature (Lond.).* 352:352–354.

Homsher, E., F. Wang, and J. R. Sellers. 1992. Factors affecting movement of F-actin filaments propelled by skeletal muscle heavy meromyosin. *Am. J. Physiol.* 262:C714-C723.

Houadjeto, M., F. Travers, and T. Barman. 1992. Ca^{2+}-activated myofibrillar ATPase. *Biochemistry.* 31:1564–1569.

Huxley, A. F. 1957. Muscle structure and theories of contraction. *Progr. Biophys.* 7:255–318.

Huxley, A. F., and R. M. Simmons. 1971. Proposed mechanism of force generation in striated muscle. *Nature (Lond.).* 233:533–538.

Ishijima, A., T. Doi, K. Sakurada, and T. Yanagida. 1991. Sub-piconewton force fluctuations of actomyosin in vitro. *Nature (Lond.).* 352:301–306.

Johnson, K. A., and E. W. Taylor. 1978. Intermediate states of subfragment 1 and actosubfragment 1 ATPase. *Biochemistry.* 17: 3437–3442.

Kawai, M., and H. R. Halvorson. 1989. Role of MgATP and MgADP in the cross-bridge kinetics in chemically skinned rabbit psoas fibers. *Biophys. J.* 55:591-603.

Kouyama, T., and K. Mihashi. 1981. Fluorimetry study of *N*-(1-pyrenyl) iodoacetamide-labelled F-actin. *Eur. J. Biochem.* 114:33–3

Lymn, R. W., and E. W. Taylor. 1971. Mechanism of adenosine triphosphate hydrolysis by actomyosin. *Biochemistry.* 10:4617–4624.

Millar, N. C., and M. A. Geeves. 1983. The limiting rate of the ATP-mediated dissociation of actin from rabbit skeletal muscle myosin subfragment 1. *FEBS Lett.* 160:141–148.

Millar, N. C., and E. Homsher. 1990. Effect of phosphate and calcium on force generation in glycerinated rabbit skeletal muscle fibers. *J. Biol. Chem.* 265:20234–20240.

Ohno, T., and T. Kodama. 1991. Kinetics of ATP hydrolysis by shortening myofibrils from psoas muscle. *J. Physiol. (Lond.).* 441:685–702.

Pate, E., and R. Cooke. 1989a. A model of cross-bridge action. *J. Muscle Res. Cell Motil.* 10:181–196.

Pate, E., and R. Cooke. 1989b. Addition of phosphate to active muscle fibers probes states within the power stroke. *Pfluegers Arch.* 414:73–81.

Pate, E., K. Franks-Skiba, H. White, and R. Cooke. 1993a. Use of differing nucleotides to investigate cross-bridge kinetics. *J. Biol. Chem.* 268:10046–10053.

Pate, E., H. White, and R. Cooke. 1993b. Determination of the myosin step size from mechanical and kinetic data. *Proc. Natl. Acad. Sci. USA.* 90: 2451–2455.

Rosenfeld, S. S., and E. W. Taylor. 1984a. The ATPase mechanism of skeletal and smooth muscle acto-subfragment 1. *J. Biol. Chem.* 259:11908–11919.

Rosenfeld, S. S., and E. W. Taylor. 1984b. Reaction of 1-N^6-ethenonucleotides with myosin subfragment 1 and acto-subfragment 1 of skeletal and smooth muscle. *J. Biol. Chem.* 259:11920–11929.

Rosenfeld, S. S., and E. W. Taylor. 1987. Mechanism of regulation of actomyosin subfragment 1 ATPase. *J. Biol. Chem.* 262:9984–9993.

Sadhu, A., and E. W. Taylor. 1992. Kinetic study of the kinesin ATPase. *J. Biol. Chem.* 267:11352–11359.

Schoenberg, M. 1988. Characterization of the myosin adenosine triphosphate cross-bridge in rabbit and frog skeletal muscle. *Biophys. J.* 54: 135–148.

Siemankowski, R. F., M. O. Wiseman, and H. D. White. 1985. ADP dissociation from actomyosin subfragment 1 is sufficiently slow to limit the unloaded shortening velocity in vertebrate muscle. *Proc. Natl. Acad. Sci. USA.* 82:658–662.

Sleep, J. A., and H. Glyn. 1986. Inhibition of myofibrillar and actomyosin subfragment 1 ATPase by ADP, pyrophosphate and adenyl-5′-yl imidodiphosphate. *Biochemistry.* 25:1149–1154.

Sleep, J. A., and R. L. Hutton. 1980. Exchange between inorganic phosphate, and adenosine 5′ triphosphate in the medium by actomyosin subfragment 1. *Biochemistry.* 19:1276–1283.

Stehle, R., T. Kraft, and B. Brenner. 1993. Stiffness speed relation for isometric and isotonic contraction. *Biophys. J.* Abs. 64:A250.

Sutoh, K., and W. F. Harrington. 1977. Cross-linking of myosin thick filaments under activating and rigor conditions. *Biochemistry.* 16: 2441–2449.

Tawada, K., and K. Sakimoto. 1991. A physical model of ATP-induced actin-myosin movement in vitro. *Biophys. J.* 59:343–356.

Taylor, E. W. 1977. Transient phase of ATP hydrolysis by myosin, heavy meromyosin and subfragment 1. *Biochemistry.* 17:732–740.

Taylor, E. W. 1989. Actomyosin ATPase Mechanism and Muscle Contraction in Muscle Energetics. R. J. Paul, G. Elzinga, and K. Yamada, editors. Alan R. Liss, New York. 9–14.

Taylor, E. W. 1991. Kinetic studies of the association and dissociation of myosin subfragment 1 and actin. *J. Biol. Chem.* 266:294–302.

Uyeda, T. Q. P., S. J. Kron, and J. A. Spudich. 1990. Myosin step size estimation from slow sliding movement of actin over low densities of heavy meromyosin. *J. Mol. Biol.* 214:699–710.

Uyeda, T. Q. P., H. M. Warrick, S. J. Kron, and J. A. Spudich. 1991. Quantized velocities at low myosin densities in an in vitro motility assay. *Nature.* 352:307–311.

White, H. D. 1985. Kinetics of tryptophan fluorescence enhancement of myofibrils. *J. Biol. Chem.* 260:982–986.

White, H. D., B. Belknap, and W. Jiang. 1993. Kinetics of binding and hydrolysis of s series of nucleoside triphosphates by actomyosin-S 1. *J. Biol. Chem.* 268:10039–10045.

Yates, L. D., and M. L. Greaser. 1983. Quantitative determination of myosin and actin in rabbit skeletal muscle. *J. Mol. Biol.* 168:123–141.24.

Yu, L. C., and B. Brenner. 1989. Structure of actomyosin cross-bridges in relaxed and rigor muscle fibers. *Biophys. J.* 55:441–453.